ELSEVIER

Contents lists available at ScienceDirect

Environmental Modelling and Software

journal homepage: www.elsevier.com/locate/envsoft





Post-processing R tool for SWAT efficiently studying climate change impacts on hydrology, water quality, and crop growth

Beibei Ding ^{a,1}, Haipeng Liu ^{a,1}, Yingxuan Li ^a, Xueliang Zhang ^a, Puyu Feng ^a, De Li Liu ^{b,c}, Gary W. Marek ^d, Srinivasulu Ale ^e, David K. Brauer ^d, Raghavan Srinivasan ^f, Yong Chen ^{a,*}

- ^a College of Land Science and Technology, China Agricultural University, Beijing, 100193, China
- ^b NSW Department of Primary Industries, Wagga Wagga Agricultural Institute, Wagga Wagga, NSW, 2650, Australia
- ^c Climate Change Research Centre, University of New South Wales, Sydney, 2052, Australia
- ^d USDA-ARS Conservation and Production Research Laboratory, Bushland, TX, 79012, USA
- e Texas A&M AgriLife Research and Extension Center at Vernon, Vernon, TX, 76384, USA
- f Department of Ecosystem Science and Management, Texas A&M University, College Station, TX, 77843, USA

ARTICLE INFO

Keywords: SWAT-MAD CMIP6 Hydrologic cycle Total nitrogen load Cotton Semi-arid region

ABSTRACT

Soil and Water Assessment Tool (SWAT) is widely used for watershed-scale assessment of climate change impacts, but post-processing of model outputs is a tedious job. An R tool was developed in this study for batch processing of SWAT output results. A case study was then performed in the Double Mountain Fork Brazos watershed in the Texas Panhandle using an improved SWAT model with the R tool to evaluate the simulated future changes in water balance components, total nitrogen (TN) load, and crop growth over the watershed. The results showed that the average annual future surface runoff increased by $8.9-17.9\,\mathrm{mm}$ and $11.5-22.6\,\mathrm{mm}$ in the irrigated and dryland cotton areas, respectively. Similarly, future TN load in irrigated and dryland cotton areas increased by approximately $0.4-0.9\,\mathrm{kg}\,\mathrm{ha}^{-1}$ and $1.9-2.4\,\mathrm{kg}\,\mathrm{ha}^{-1}$. The yields of irrigated and dryland cotton increased by 91.1%-122.1% and 47.5%-84.0% under the future climate scenarios, respectively.

1. Introduction

Climate change is expected to present critical challenges for supply chain and production systems throughout the world (Papadopoulos and Balta, 2022). Changes in climatic conditions and the occurrence of extreme climatic events can have a substantial impact on the water, ecological, and agricultural resources (Arnell and Reynard, 1996). The average global surface temperature has increased by approximately 1 °C since 1850 (Intergovernmental Panel on Climate Change; IPCC, 2014). Climate warming accelerates the regional water cycle processes, causing the spatio-temporal redistribution of water resources. This also leads to changes in water resources availability, which in turn leads to changes in hydrological regimes and further impacts on regional socio-economic systems (Gleick, 1989; Al-Mukhtar et al., 2014). At the same time, climate change also aggravates the occurrence of extreme weather events, such as drought, flooding, etc., and thereby directly affects crop growth and development. The extremely high temperatures could reach the critical tolerance threshold of crop health. Extreme drought could

result in water stress and induce a series of problems such as yield reduction or crop failure (Wing et al., 2021; Vesco et al., 2021; Kukal and Irmak, 2018). In addition, with the changes in rainfall-runoff relationships, the generation and migration of pollutants with the hydrologic cycle as the carrier and the driving force will also vary (Zhang et al., 2021a; Wagner-Riddle et al., 2017), which can seriously threaten crop growth and environmental quality. Therefore, assessing the impact of climate change is of immense significance for effectively preventing the destruction of the agricultural environment of a basin and optimizing the management practices for soil and water conservation.

Scenario construction is the foundation of climate change modeling, assessing climate change impacts and vulnerabilities, evaluating adaptation and mitigation strategies, and analyzing climate change related policies (Nakićenović, 1996). A physically-based distributed hydrological model not only considers the spatial heterogeneity of the watershed but also accurately describes the hydrological process of the watershed. It can effectively simulate the long-term impact of climate change and land use conversion in a watershed and perform continuous simulation,

^{*} Corresponding author.

E-mail address: yongchen@cau.edu.cn (Y. Chen).

¹ Beibei Ding and Haipeng Liu contributed equally to this paper.

and therefore, it is appropriate for watersheds with large differences in spatial characteristics (Abbott and Refsgaard, 1996). The Soil and Water Assessment Tool (SWAT) model is used extensively and effectively for simulating water quantity and quality in different watersheds around the world (Hosseini and Bailey, 2022; Samimi et al., 2020; Kuti and Ewemoje, 2021). The model discretizes the watershed in various ways to represent the spatial heterogeneity and hydrological processes of the watershed. At a daily time step, SWAT can well simulate the impact of climate change on the watershed-scale hydrological cycle (Neitsch et al., 2009; Arnold et al., 2012). Recently, SWAT has been extensively used to evaluate hydrological and water quality responses to climate variability and land use change. Marras et al. (2021) utilized the coupled EURO-CORDEX and SWAT model to show decreases in mean discharge and runoff due to decreased precipitation. Son et al. (2022) found that all hydrological components were decreased (such as evapotranspiration by -2.3%, percolation by -9.8%, and surface runoff by -11.5%) under climate change scenarios, and evapotranspiration (ET) and surface runoff were the most sensitive hydrological parameters in the future. Wang et al. (2020) examined responses of nitrate loading to climate change in the Upper Mississippi River Basin using an improved SWAT model with Freeze-Thaw cycle representation (SWAT-FT) and found that the SWAT-FT model simulated approximately a 50% increase in riverine nitrate loadings under the RCP8.5 scenario. Tan et al. (2022) utilized an improved SWAT model and simulated that yields of winter wheat (10.0-17.1%) and summer maize (6.1-12.6%) could increase in the future under SSP2-4.5 and SSP5-8.5 scenarios in the middle (2041–2070) and end (2071–2100) of 21st century, respectively.

When assessing the impacts of climate change using hydrological models and general circulation models (GCMs), uncertainty in the simulated hydro-climatic variables is inevitable (Wilby and Harris, 2006). GCM credibility plays a significant role in the robustness of system modeling and decision-making. Downplaying GCM credibility may lead to over or under estimation in future scenarios, leading to biased climate change adaptation decisions (Zhang et al., 2021b). Thereby, choosing a single or several GCMs to analyze climate change neither covers enough uncertainties nor guarantees the reliability of the results (Mehr et al., 2020). Taking into account the uncertainty of GCM climate data, for example, Shen et al. (2018) predicted future changes in both climate (precipitation and air temperature) and the hydrological responses of the Hanjiang River watershed based on 20 different GCMs, and found that the uncertainty increased dramatically over time. Based on the data from 28 GCMs for the Manicouagan Basin, Chen et al. (2017) reported an increase in precipitation from 9.7% to 27.8%, and an increase in air temperature from 3.8 °C to 8.4 °C under RCP8.5 scenario. These studies demonstrated the importance of using data from multiple GCMs to evaluate the impacts of climate change on hydrology (Lee et al., 2021). Predictions from an ensemble of multiple models can reduce the uncertainty of simulation results (Faramarzi et al., 2013; Asseng et al., 2019; Yun et al., 2021). Therefore, 27 GCMs were selected from different countries and regions in this study.

Coupled Model Intercomparison Project (CMIP) has been rigorously refined over the years to address uncertainties, from CMIP1 to the latest version of CMIP6 (O'Neill et al., 2016). Unlike previous CMIPs, the CMIP6 includes more GCMs and provides a more accurate description of geophysical processes. In addition, the future climate change scenarios in CMIP6 provide data for combined scenarios of Representative Concentration Pathways (RCPs) used in CMIP5 and Shared Socioeconomic Pathways (SSPs) (O'Neill et al., 2016; Schlund et al., 2020), which consider future social and economic developments. And, CMIP6 added 3 new emission paths, which greatly enriched the future climate database. When such huge meteorological data are invoked as the input data for SWAT to simulate the future hydrology, water quality, and crop growth, large output data becomes available. Manual processing of such massive data is not only time-consuming and labor-intensive, but also prone to accidental errors. Currently available data processing methods limit the availability of climate scenarios and GCMs to be used for some studies.

In response to this challenge, in this study, R code was developed to design an algorithm specifically used for post-processing the SWAT output data (output.hru) at daily, monthly, and yearly time scales. This algorithm can quickly extract the required variables and organize them into CSV files for further use.

The Double Mountain Fork Brazos (DMFB) watershed in the semiarid Texas Panhandle was selected for this case study. Cotton (Gossypium hirsutum L.) land use accounts for approximately 30% of the study watershed area and approximately 40% of this cotton area is irrigated (National Agricultural Statistics Service; NASS, 2021). The Ogallala Aquifer serves as an important groundwater source for cotton irrigation. However, decades of intensive irrigation pumping combined with limited recharge have led to rapidly declining water levels (Colaizzi et al., 2009). Therefore, understanding the status of water resources in this region under global warming is of profound significance for developing appropriate management practices for cotton production. In this study, the downscaled CMIP6 meteorological data were used to drive an improved SWAT model. The impacts of projected future climate change on major water balance components, water quality, and cotton yield in the DMFB watershed were assessed. The specific objectives of the study were to: (1) develop an algorithm for rapidly post-processing SWAT output data; (2) assess the long-term climate change effects on the hydrologic cycle and total nitrogen load in the DMFB watershed under both irrigated and dryland cotton land uses; and (3) evaluate how the projected climate change affects the irrigated and dryland cotton production.

2. Materials and methods

2.1. Study area

This study was conducted in the DMFB watershed in the semi-arid Texas Panhandle. The delineated area of this watershed is approximately $6000\,\mathrm{km}^2$. The topography of the watershed is fairly flat. It is situated above the southern Ogallala Aquifer and more than 90% of agricultural irrigation in the area relies on this groundwater extraction. Cotton is a dominant crop, and cotton production holds enormous potential in this region. In general, cotton is planted around mid-May and harvested around the end of October in the Texas Panhandle. Defoliant is typically applied two weeks before harvesting when needed. The long-term average annual rainfall across the watershed varies between 457 and 559 mm, and the long-term average annual maximum air temperature (T_{max}) and minimum air temperature (T_{min}) are approximately 24 °C and 9 °C, respectively.

2.2. SWAT and SWAT-MAD

The SWAT model is a continuous-time, semi-distributed, process-based, and watershed-scale hydrologic model (Arnold et al., 1998). Primary components include a hydrology module, non-point source pollution module, crop growth module, etc. (Arnold et al., 2012). The ArcSWAT (revision 664) developed for the ArcGIS 10.2 platform was used in this study.

Irrigation in HRUs may be scheduled manually by users or automatically applied by SWAT (Neitsch et al., 2011). Chen et al. (2018a) developed a more representative approach to automatically schedule irrigation and integrated a management allowed depletion (MAD) auto-irrigation method into the SWAT model. The MAD method triggers irrigation according to a user-defined allowable depletion percentage of plant available water, determined by the crop-specific maximum rooting depth and site-specific soil properties (Chen et al., 2018a).

MAD method:
$$(sol_sumfc - sol_sw) / PAW > MAD$$
 (1)

where sol_sumfc is the amount of water held in the soil profile at field capacity (mm); sol_sw is the amount of water stored in soil profile on any

given day (mm); PAW is plant available water, determined by both plant maximum rooting depth and soil properties; and MAD is users defined water stress threshold that triggers irrigation, which expressed as a decimal value ranging from 0 to 1. MAD values approaching 0 indicate irrigation management that allows relatively less depletion of soil water before triggering irrigation, resulting in low crop water stress. By contrast, values approaching 1 denote irrigation management that allows relatively more depletion of soil water before applying irrigation, leading to high crop water stress.

In this study, the SWAT-MAD model was calibrated and validated for streamflow data at two United States Geological Survey (USGS) gages and county-level crop yields of both irrigated and dryland cotton. The SWAT-MAD model was also evaluated by county-level seasonal irrigation requirements of cotton and percolation amount. The total nitrogen (TN) load at the watershed outlet was also calibrated and validated in this study. The calibrated parameter values for the SWAT-MAD model are listed in Table S1. The SWAT-MAD model calibration and validation performance statistics for monthly streamflow at the stream gages (Table 1) were well above the "satisfactory" range suggested by Moriasi et al. (2007). The R^2 and overall PBIAS were 0.21 and 2.3% when comparing SWAT-MAD simulated and observed irrigated cotton lint vield in Lynn County in the DMFB watershed (NASS, 2020). The simulated irrigation for cotton by the MAD auto-irrigation method (346.9 mm) was very close to the local survey data of 345.4 mm (NASS, 2020). The SWAT-MAD model simulated percolation amount was also comparable with the values from local reports and literature (Chen et al., 2018b). The NSE, R^2 , and PBIAS for monthly TN load prediction at the watershed outlet during the calibration period were 0.72, 0.75, and −13.8%, respectively (Table 1). Those values during the validation were 0.73, 0.88, and 17.0%. The model performance ratings for the monthly TN load simulations using SWAT-MAD in the DMFB watershed were considered good for both the calibration and validation periods according to Moriasi et al. (2007) criteria.

2.3. CMIP6 GCM data and scenario design

Observed daily climate data for the study watershed, including T_{max} , T_{min} , solar radiation, and precipitation from 1981 to 2010 were obtained for seven weather stations from the Iowa Environmental Mesonet (https://mesonet.agron.iastate.edu/schoolnet/). Future climate scenario data were obtained from 27 GCMs, which are provided by the World Climate Research Program (WCRP) of CMIP6 (https://esgf-node.llnl.gov/project

Table 1Performance statistics for monthly predictions of streamflow and total nitrogen load in the Double Mountain Fork Brazos watershed using the SWAT-MAD model

| Streamflow | Gage I | | Gage II | | |
|--|-------------------------|----------------|------------------------|----------------|--|
| | Calibration | Validation | Calibration | Validation | |
| | (1994–2001) | (2002–2009) | (1994–2001) | (2002–2009) | |
| Nash- | 0.86 (Very | 0.59 | 0.63 | 0.64 | |
| Sutcliffe efficiency (NSE) | good ^a) | (Satisfactory) | (Satisfactory) | (Satisfactory) | |
| R^2 | 0.88 | 0.71 | 0.67 | 0.75 | |
| Percent bias | 14.6 | 8.5 | 12.9 | -12.6 | |
| (PBIAS; %) | (Good) | (Very good) | (Good) | (Good) | |
| Total nitrogen load ^b | Calibration (1995–1997) | | Validation (1998–2000) | | |
| NSE | 0.72 (Good) | | 0.73 (Good) | | |
| R^2 | 0.75 | | 0.88 | | |
| PBIAS | -13.8 (Very good) | | 17.0 (Very good) | | |

^a General model performance ratings suggested by Moriasi et al. (2007) for monthly predictions of streamflow and nitrogen.

s/cmip6/). The raw GCMs from WCRP were in low spatial and temporal resolutions, hence the downscaled and bias-corrected methods developed by Liu and Zuo (2012) were used to generate the daily datasets. The 27 CMIP6 GCMs were listed in Table 2.

In this study, the water balances, TN load, and crop growth attributes of the watershed under climate change scenarios in the mid-21st century and the end of the 21st century were simulated. Two 35-year periods (from 2036 to 2070 and from 2066 to 2100) were selected to conduct future scenario simulations forced with both SSP2-4.5 and SSP5-8.5 scenarios. The first five years of 2036-2040 and 2066-2070 served as the warmup periods. The CO2 concentration in SWAT was modified while inputting future climate data. The current version of SWAT does not allow inputting variable CO2 concentration values that change dynamically with time, and it allows only a fixed value for a period of simulation. Therefore, according to Meinshausen et al. (2011) and Van Vuuren et al. (2007), the 35-year average CO₂ concentrations of the future climate scenarios (SSP2-4.5 and SSP5-8.5) in each of the two time periods were estimated and used as the CO2 concentrations in the SWAT-MAD model. The CO₂ concentration in the historical period was kept as the default value of 330 ppm. The average CO₂ concentrations in the two time periods under the two SSP scenarios were shown in Table 3.

2.4. Overall R framework design

In this study, post-processing R codes were developed for batch processing of SWAT outputs of the future climate change scenarios. The R code intellectualized the SWAT output post-processing procedure compared to the conventional manual processing, allowing for flexibility to obtain the climate, hydrological, water quality, and crop growth variables of the SWAT model from output.hru for different time steps (daily, monthly, and yearly). In this study, climatic variables, hydrological variables, TN load, and crop yield could be obtained from the monthly output.hru results, while the dynamic change of biomass (BIOM) and leaf area index (LAI) had to be obtained from the daily output.hru results. The monthly output.hru file of the SWAT model included both monthly and yearly results, so the yearly simulation results were not needed to output separately using the newly developed R code. The future climate data of 27 GCMs for two time periods and two

Table 2List of 27 CMIP6 general circulation models (GCMs) considered in the study.

| Model ID | Name | Abbreviation | Institution ID | Country |
|----------|-----------------|--------------|----------------|-----------|
| 01 | ACCESS-CM2 | ACC1 | BoM | Australia |
| 02 | ACCESS-ESM1-5 | ACC2 | BoM | Australia |
| 03 | BCC-CSM2-MR | BCCC | BCC | China |
| 04 | CanESM5 | Can1 | CCCMA | Canada |
| 05 | CanESM5-CanOE | Can2 | CCCMA | Canada |
| 06 | CIESM | CIES | THU | China |
| 07 | CMCC-CM2-SR5 | CMCS | CMCC | Europe |
| 08 | CNRM-CM | CNR1 | CNRM | France |
| 09 | CNRM-CM6-1-HR | CNR2 | CNRM | France |
| 10 | CNRM-ESM | CNR3 | CNRM | France |
| 11 | EC-Earth3 | ECE1 | EC-EARTH | Europe |
| 12 | EC-Earth3-Veg | ECE2 | EC-EARTH | Europe |
| 13 | FGOALS-g3 | FGOA | FGOALS | China |
| 14 | GFDL-ESM4 | GFD1 | NOAA GFDL | America |
| 15 | GFDL-CM4 | GFD2 | NOAA GFDL | America |
| 16 | GISS-E2-1-G | GISS | NASA GISS | America |
| 17 | HadGEM3-GC31-LL | HadG | MOHC | Britain |
| 18 | INM-CM4-8 | INM1 | INM | Russia |
| 19 | INM-CM5-0 | INM2 | INM | Russia |
| 20 | IPSL-CM6A-LR | IPSL | IPSL | France |
| 21 | MIROC6 | MIR1 | MIROC | Japan |
| 22 | MIROC-ES2L | MIR2 | MIROC | Japan |
| 23 | MPI-ESM1-2-HR | MPI1 | MPI-M | Germany |
| 24 | MPI-ESM1-2-LR | MPI2 | MPI-M | Germany |
| 25 | MRI-ESM2-0 | MRIE | MRI | Japan |
| 26 | NESM3 | NESM | NUIST | China |
| 27 | UKESM1-0-LL | UKES | Met Office | Britain |

^b The number of observed data used in the LOADEST estimation for total nitrogen loads were 39 samples at the watershed outlet.

Table 3Description of the future climate change scenarios.

| Periods | SSPs | CO ₂ concentration (ppm) |
|-------------------------------|-----------------------|-------------------------------------|
| Historical period (1981–2010) | _ | 330 |
| 2041-2070 | SSP2-4.5 ^a | 497 |
| 2071-2100 | SSP2-4.5 | 533 |
| 2041-2070 | SSP5-8.5 ^a | 578 |
| 2071-2100 | SSP5-8.5 | 807 |

^a SSP2-4.5: radiative forcing of $4.5~W~m^{-2}$ and mid-range emission; SSP5-8.5: radiative forcing of $8.5~W~m^{-2}$ and high-end emission (O'Neill et al., 2016).

SSP scenarios were inputted into SWAT-MAD first. In addition, the SWAT-MAD projects were run at both the monthly and daily scales, and a total of 218 output.hru files were obtained. All output.hru files were renamed according to the user's need (naming example is shown in Figs. S1–S2) and then saved into two folders for monthly scale and daily scale, separately.

As for how the R tool functions, firstly, the function determined the position information of the output variable (Fig. 1). The 'MON' column was used to distinguish results between monthly, yearly, and multi-year totals because the monthly scale output contained information on all three aspects. Specifically, when 'MON' column values are greater than 999, they were identified as yearly scale results (simulation starting year, in this case, needs to be greater than 1000 A.D.). When the value of the 'MON' column was less than or equal to 12 and the row ordinal number was less than that of the last row for the yearly scale results, monthly scale results were obtained this way. The row ordinal of the 'MON' column, starting from the first row below the last row ordinal of the yearly scale results to the end of all results in the output.hru file, was the multi-year summary results (Appendix S1). For the daily scale results, the values of the 'MON' column represented the day of the year (DOY). Since the LAI and biomass values on the 366th day were 0 for cotton, the values on the 366th day of a leap year were deleted at the daily scale, which was conducive to the smooth operation of the code (Appendix S2). The R codes read all ".hru" files in the folders for monthly scale and daily scale, and cycled through all files in the order of "file name acquisition - read data - data filtering - save data". Finally, the results for each time scale of 27 GCMs were combined into an independent CSV file for further data analysis or chart making (Fig. 1).

3. Results

3.1. Projected changes in the future climate of the watershed

Overall, the long-term changes in annual Tmax, Tmin, and solar radiation showed increasing trends in the DMFB watershed from 2041 to 2100 (Tables S2-S3). But the projected changes of annual precipitation were relatively small, with the mean and median percent changes of less than 3% (Fig. 2). Especially under the 2071-2100 SSP5-8.5 scenario, the mean percent changes in annual precipitation for irrigated and dryland cotton production areas were 1.5% and 1.2%, and the median percent changes were 2.7% and 2.0%, respectively (Fig. 2). This study revealed that the average annual precipitation gradually increased with increasing CO₂ concentrations, while the average annual solar radiation decreased. In contrast to the SSP2-4.5 scenario, the SSP5-8.5 scenario showed a greater uncertainty in predicted future climate parameters for different time scales. Compared to the baseline period (1981–2010), the average annual precipitation during the growing season was projected to increase by 2.0% for irrigated cotton areas and 1.7% for dryland cotton areas during 2041-2070, and those increases were 5.0% and 4.7% during 2071–2100 (Figs. S3–S4). The average annual T_{max} during the growing season for irrigated cotton is expected to increase by $2.03\,^{\circ}$ C, $2.62\,^{\circ}$ C, $2.67\,^{\circ}$ C, and $4.55\,^{\circ}$ C, and the average annual T_{min} is projected to increase by 1.97 °C, 2.68 °C, 2.62 °C, and 4.89 °C under the 2041-2070 SSP2-4.5, 2041-2070 SSP5-8.5, 2071-2100 SSP2-4.5, and 2071-2100 SSP5-8.5 scenarios, respectively (Figs. S5 and S7). The mean annual T_{max} for the dryland cotton growing period could rise by 2.44 °C and 3.71 $^{\circ}$ C, and the mean annual T_{min} could rise by 2.47 $^{\circ}$ C and 4.07 $^{\circ}$ C during the period of 2041-2100 under two emission scenarios (Table 4; Figs. S6 and S8). For both cotton management practices, the increases in solar radiation were greater under the SSP2-4.5 scenario than the SSP5-8.5 scenario. The median percent changes in solar radiation during the growing season under the SSP2-4.5 and SSP5-8.5 scenarios were 0.6% and 0.2% for irrigated cotton, and 0.7% and 0.2% for dryland cotton, respectively (Table 5; Figs. S9–S10).

3.2. Climate change impacts on hydrology

The annual actual evapotranspiration (ET $_a$) for dryland cotton was projected to decrease during 2041–2100 under two SSP scenarios. For irrigated cotton, only the 2071–2100 SSP5-8.5 scenario showed a 9.3% decrease in the mean annual ET $_a$, whereas the rest of the scenarios showed slight increases (Fig. 3). A high variation in annual ET $_a$ was

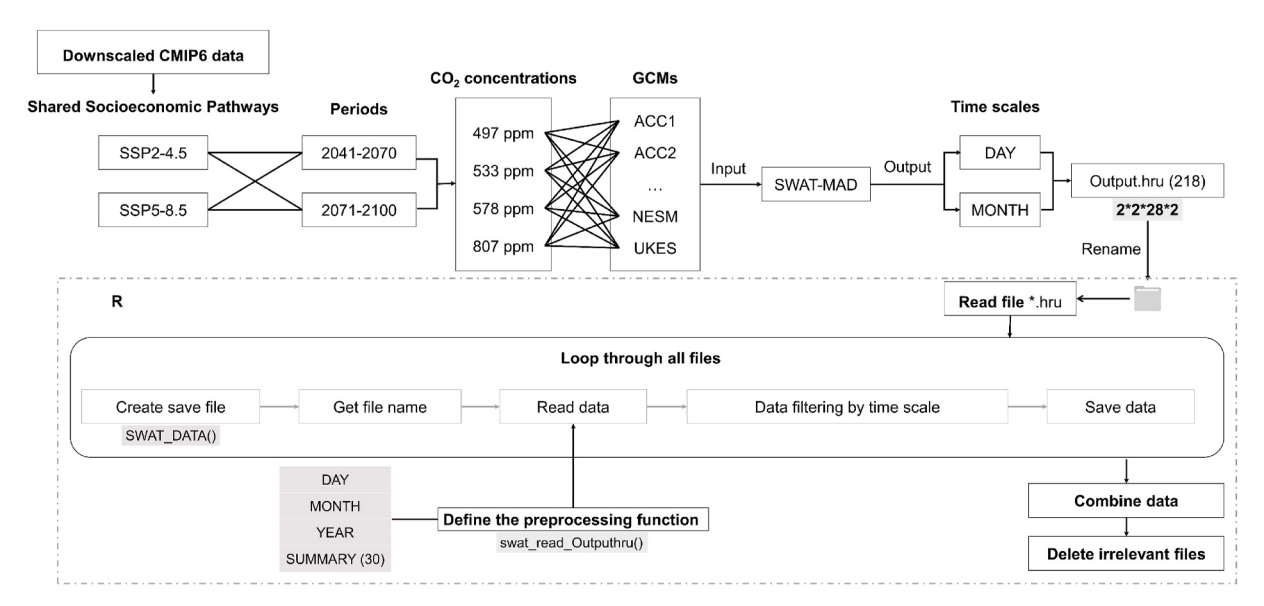


Fig. 1. Flowchart of post-processing R tool for SWAT output.hru processing.

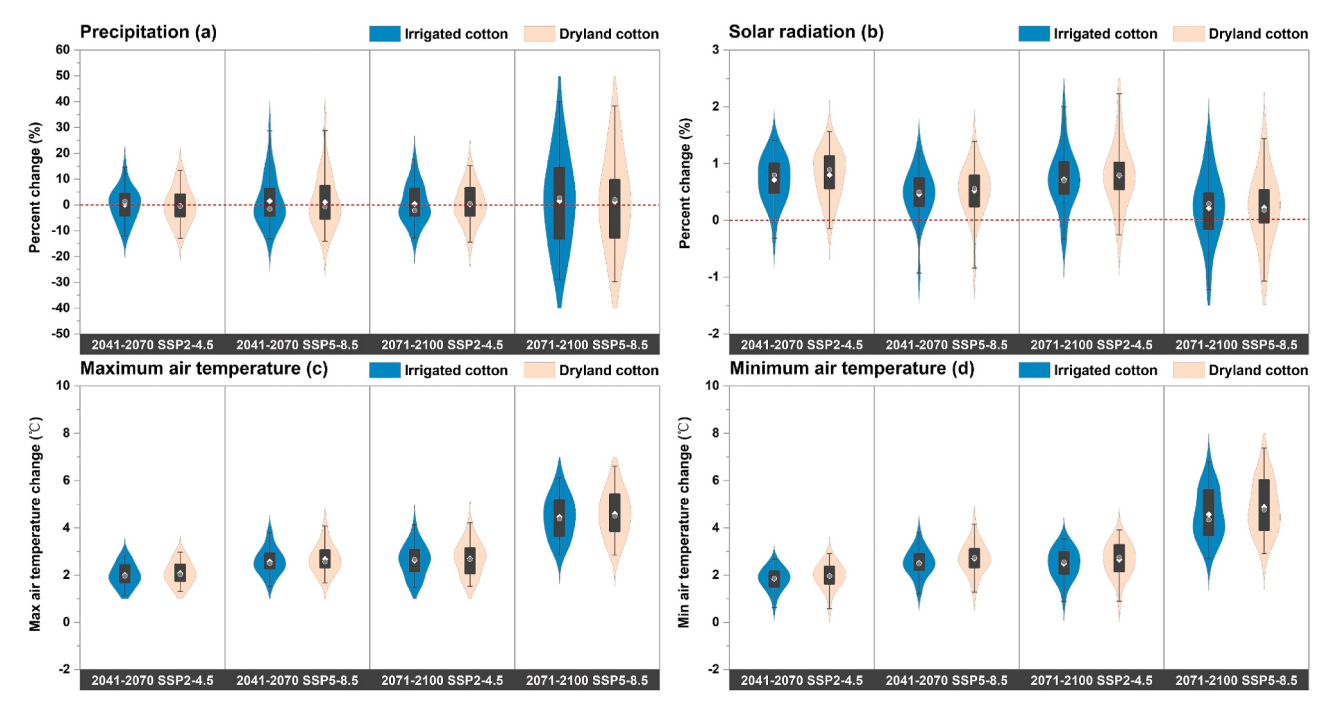


Fig. 2. Changes in precipitation (a), solar radiation (b), maximum air temperature (c), and minimum air temperature (d) between future and historical periods for 27 GCM models. The blue plots display trends for irrigated cotton and the yellow plots display trends for dryland cotton. Average changes are shown by solid circles, the medians are represented by solid diamonds, whereas minimum, first quartile, third quartile, and maximum are presented as violin plots.

Table 4 Mean and Median changes in maximum air temperature (T_{max}), minimum air temperature (T_{min}), surface runoff, and total nitrogen load during the cotton growth period from 2041 to 2100.

| Scenarios | Cotton | Statistic | T _{max} / °C | T _{min} / °C | Surface runoff/ mm | Total nitrogen load/kg ha ⁻¹ |
|-----------|-----------|-----------|--------------------------|--------------------------|--------------------------|--|
| SSP2-4.5 | Irrigated | Mean | 2.35 | 2.30 | 1.5 | 0.1 |
| | | Median | 2.29 | 2.24 | 0.4 | 0.0 |
| | Dryland | Mean | 2.44 | 2.47 | 2.0 | 0.3 |
| | | Median | 2.40 | 2.40 | 1.0 | 0.1 |
| SSP5-8.5 | Irrigated | Mean | 3.59 | 3.78 | 2.4 | 0.1 |
| | | Median | 3.31 | 3.36 | 0.9 | 0.0 |
| | Dryland | Mean | 3.71 | 4.07 | 3.1 | 0.4 |
| | | Median | 3.48 | 3.64 | 1.5 | 0.2 |

found among different GCMs, especially under the SSP5-8.5 scenario, the percent changes in annual $\rm ET_a$ ranged from -4.1% to -13.9% for irrigated cotton and -29.5% to 29.4% for dryland cotton during 2071–2100 (Fig. 3). Based on the future climate data projected by 27 GCMs, the results showed greater uncertainty under dryland conditions than under irrigated conditions. The $\rm ET_a$ indicated a higher level of uncertainty during April and September for both cotton management

practices. The projected changes in mean and median ET_a during the growing season for irrigated cotton ranged from -13.4% to 1.4% and -11.2%-1.9%, respectively. The decrease in mean and median ET_a during the growing season for dryland cotton varied from 5.1 to 7.9% and 2.9%-8.1%, respectively (Figs. S11–S12). The future irrigation water use showed similar increasing trends under all scenarios, except for the 2071-2100 SSP5-8.5 scenario, in which the median percent change in irrigation water use was -17.5% (Fig. 3). Nevertheless, the magnitude of change in irrigation water use during the cotton growing season was slightly larger, with values of 5.6%, 2.5%, and 6.8%, under the 2041-2070 SSP2-4.5, 2041-2070 SSP5-8.5, and 2071-2100 SSP2-4.5 scenarios, respectively (Fig. S13). The change in irrigation water use decreased by 18.0% under the 2071-2100 SSP5-8.5 scenario.

The mean annual surface runoff in the DMFB watershed indicated an increasing trend under all climate change scenarios (Fig. 3). Under the 2041–2070 SSP2-4.5 and 2041–2070 SSP5-8.5 scenarios, the mean annual surface runoff increased by 8.9 mm and 13.4 mm, respectively, for irrigated cotton, and 11.5 mm and 17.8 mm, respectively, for dryland cotton. During the period of 2071–2100, the annual mean surface runoff for irrigated cotton increased by 10.1 mm under the SSP2-4.5 scenario and 17.9 mm under the SSP5-8.5 scenario, and the increased values for dryland cotton were 14.1 mm and 22.6 mm. However, the simulated surface runoff results under the SSP5-8.5 scenario exhibited substantial uncertainty for both cotton management practices. For example, the

Table 5
Change percentages (%) of Mean and Median values for precipitation, solar radiation, actual evapotranspiration, and irrigation during the cotton growing period 2041-2100.

| Scenarios | Cotton | Statistic | Precipitation | Solar radiation | Actual evapotranspiration | Irrigation |
|-----------|-----------|-----------|---------------|-----------------|---------------------------|------------|
| SSP2-4.5 | Irrigated | Mean | 2.4 | 0.6 | 1.4 | 6.2 |
| | | Median | -1.2 | 0.6 | 1.4 | 6.4 |
| | Dryland | Mean | 2.0 | 0.6 | -5.6 | - |
| | | Median | -2.2 | 0.7 | -5.5 | - |
| SSP5-8.5 | Irrigated | Mean | 4.9 | 0.1 | -6.7 | -7.7 |
| | | Median | 3.7 | 0.2 | -5.4 | -4.0 |
| | Dryland | Mean | 4.5 | 0.1 | -6.8 | - |
| | | Median | 0.9 | 0.2 | -5.5 | - |

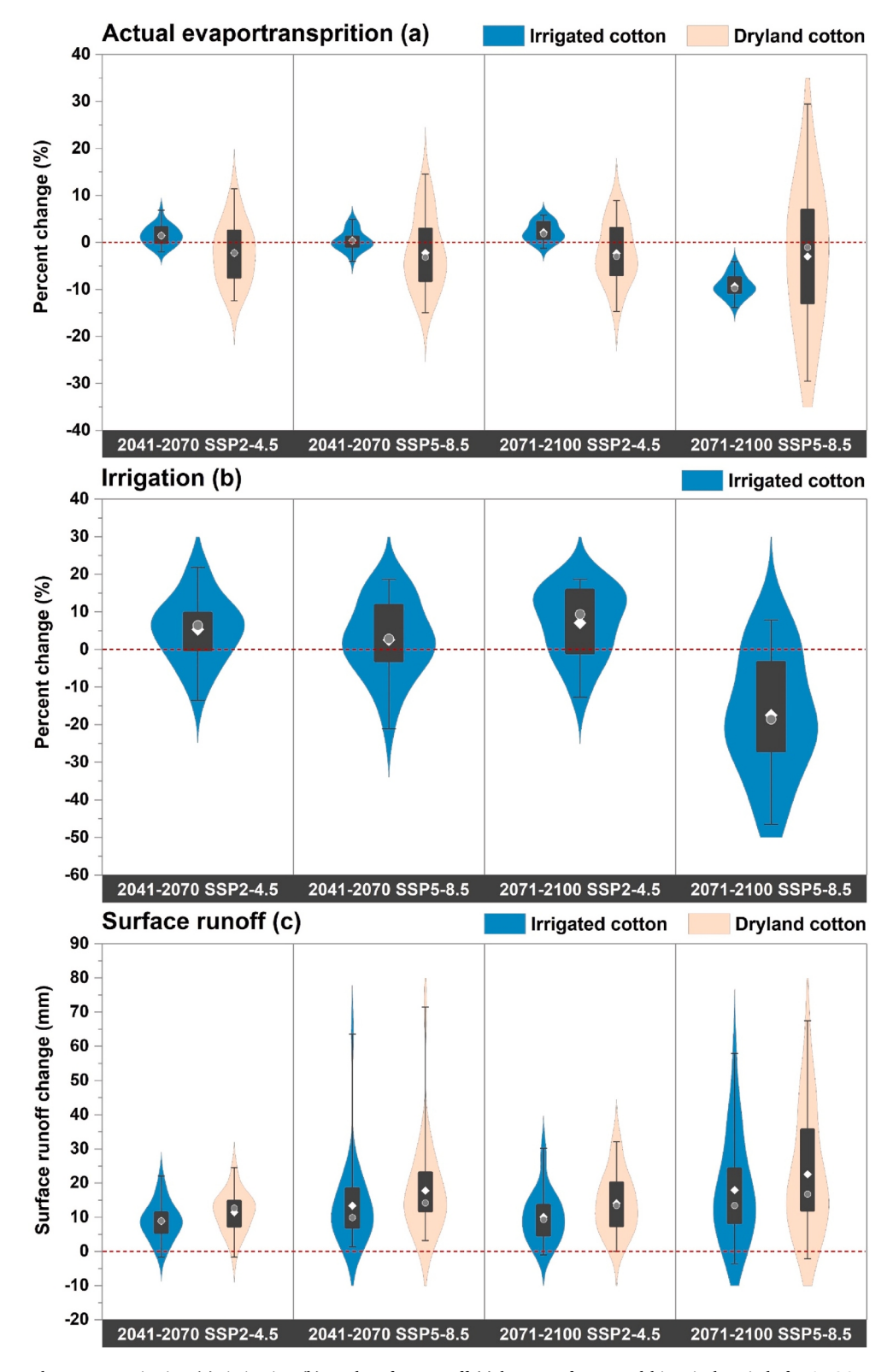


Fig. 3. Changes in actual evapotranspiration (a), irrigation (b), and surface runoff (c) between future and historical periods for 27 GCM models. The blue plots display trends for irrigated cotton and the yellow plots display trends for dryland cotton. Average changes are shown by solid circles, the medians are represented by solid diamonds, whereas minimum, first quartile, third quartile, and maximum are presented as violin plots.

projected change range in surface runoff among 27 GCMs was approximately 30 mm under the SSP2-4.5 scenario and it was over 60 mm under the SSP5-8.5 scenario (Fig. 3). Based on the monthly analysis, the change in surface runoff during the non-growing season was small and showed a low uncertainty. During the growing season, the maximum

increase in monthly surface runoff is expected to occur in September with a high uncertainty (Figs. S14–S15). The surface runoff changes during the growing season in irrigated areas could increase with increasing $\rm CO_2$ concentrations. Results also found that the average increase in annual surface runoff differed from 1.4 mm to 2.1 mm in the

mid-21st century and 1.6 mm–2.7 mm by the end of the 21st century. A similar trend was observed for dryland cotton, and the average surface runoff showed an annual increase from 1.8 mm to 2.8 mm in the mid-21st century and 2.2 mm–3.5 mm by the end of the 21st century. The above results indicated that the hydrological cycle in the DMFB watershed was strongly influenced by future climate, with a greater magnitude of changes under the SSP5-8.5 scenario.

3.3. Climate change effects on water quality

Surface runoff has been recognized as one of the common causes and transport pathways for agricultural non-point source pollution, and changes in surface runoff caused by climate change could affect the future TN load in the DMFB watershed. The simulated results for TN load were consistent with the trend of surface runoff, which showed an increasing trend in the future. Under four climate change scenarios, the mean and median TN load for irrigated cotton increased by 0.4 kg ha⁻¹ to 0.9 kg ha^{-1} and 0.3 kg ha^{-1} to 0.7 kg ha^{-1} , respectively; the mean and median annual TN load for dryland cotton ranged from 1.9 kg ha⁻¹ to 2.4 kg ha^{-1} and from 1.7 kg ha^{-1} to 2.1 kg ha^{-1} , respectively (Fig. 4). Meanwhile, the two SSP emission scenarios consistently projected increasing trends in TN load during the growing season under both irrigated and dryland conditions, and the change in TN load was negligible during the non-growing season, as expected. The mean and median change in TN load during the growing season increased from 0.06 kg ha^{-1} to 0.13 kg ha^{-1} and from 0.02 kg ha^{-1} to 0.05 kg ha^{-1} (irrigated cotton), and from $0.30~{\rm kg\,ha}^{-1}$ to $0.37~{\rm kg\,ha}^{-1}$ and from $0.10 \,\mathrm{kg} \,\mathrm{ha}^{-1}$ to $0.18 \,\mathrm{kg} \,\mathrm{ha}^{-1}$ (dryland cotton), respectively (Figs. S16-S17).

3.4. Responses of cotton yields to climate change

The future cotton lint yields, biomass, and LAI for both irrigated and dryland conditions were simulated using the SWAT-MAD model and GCM-projected future climate data. In the mid to late $21^{\rm st}$ century, under the SSP2-4.5 and SSP5-8.5 scenarios, the future cotton lint yield simulated by all GCMs changed remarkably. The simulated cotton lint yield in the DMFB watershed increased from 91.1% to 122.1% under irrigated conditions and from 47.5% to 84.0% under dryland conditions (Fig. 5). Compared to the results from the SSP2-4.5 scenario, the SSP5-8.5 scenario showed higher CO₂ concentration and greater increases in cotton lint yields. The simulated cotton lint yields under both irrigated and

dryland conditions increased by 98.4% and 50.6%, respectively, under the SSP2-4.5 scenario. The simulated percent changes in cotton lint yields under both irrigated and dryland conditions were 116.7% and 72.3%, respectively, under the SSP5-8.5 scenario (Table S3). Dry matter accumulation is the material basis for crop yield. The simulated changes in biomass approximately exhibited S-shaped curves for both irrigated and dryland cotton. The biomass could increase with increasing CO2 concentrations, and the stage of rapid biomass accumulation could occur earlier. Simulated biomass increased by 4 Mg ha $^{-1}$ to 6.4 Mg ha $^{-1}$ for irrigated cotton and 1.5 Mg ha $^{-1}$ to 2.5 Mg ha $^{-1}$ for dryland cotton under future scenarios, compared to the historical period (Fig. 5).

The simulated LAI during the baseline period (1981-2021) showed an S-shape curve. However, LAI showed a downward opening parabola during the simulation periods of 2041-2070 and 2071-2100. The simulated LAI increased rapidly in the early growth stage and reached the maximum at the full development stage. The simulated LAI was generally lower in dryland conditions than in irrigated conditions under all scenarios (Fig. 5). Under the baseline scenario ($CO_2 = 330 \text{ ppm}$), the simulated LAI leveled off around DOY 111 for irrigated cotton $(4.6 \text{ m}^2 \text{ m}^{-2})$ and around DOY 105 for dryland cotton $(2.8 \text{ m}^2 \text{ m}^{-2})$. For irrigated cotton, the LAI reached a maximum value of 4.7 m² m⁻² on DOY 108 and began to decline after 20 days under the 2041-2070 SSP2-4.5 scenario. The trends of LAI were similar under the 2071-2100 SSP2-4.5 and 2041-2070 SSP5-8.5 scenarios, which reached a maximum value of $4.6\,\mathrm{m}^2\,\mathrm{m}^{-2}$ on DOY 84 and DOY 85, respectively, and began to decline on DOY 127 and DOY 122, respectively. Under the SSP5-8.5 scenario, the simulated LAI reached a maximum value of 4.5 m² m⁻² on DOY 77 and started to decrease after one month. For dryland cotton, LAI reached a maximum value of 3.1 m² m⁻² on DOY 102 under the 2041-2070 SSP2-4.5 scenario and started to decrease after 19 days. The 2071-2100 SSP2-4.5 and 2041-2070 SSP5-8.5 scenarios simulated similar trends in LAI, which reached a maximum value of 3.1 m² m⁻² on DOY 79 and 82 and began to decline on DOY 127 and 122, respectively. The simulated LAI reached a maximum value of $3.5\,\mathrm{m}^2\,\mathrm{m}^{-2}$ on DOY 77 and started to decrease after 24 days under the 2071-2100 SSP5-8.5 scenario (Fig. 5).

4. Discussion

The CMIP6 projected air temperatures showed that the climate in the DMFB watershed could generally become warmer under most scenarios, and all 27 GCMs projected air temperature increases ranging from $1.5\,^\circ\text{C}$

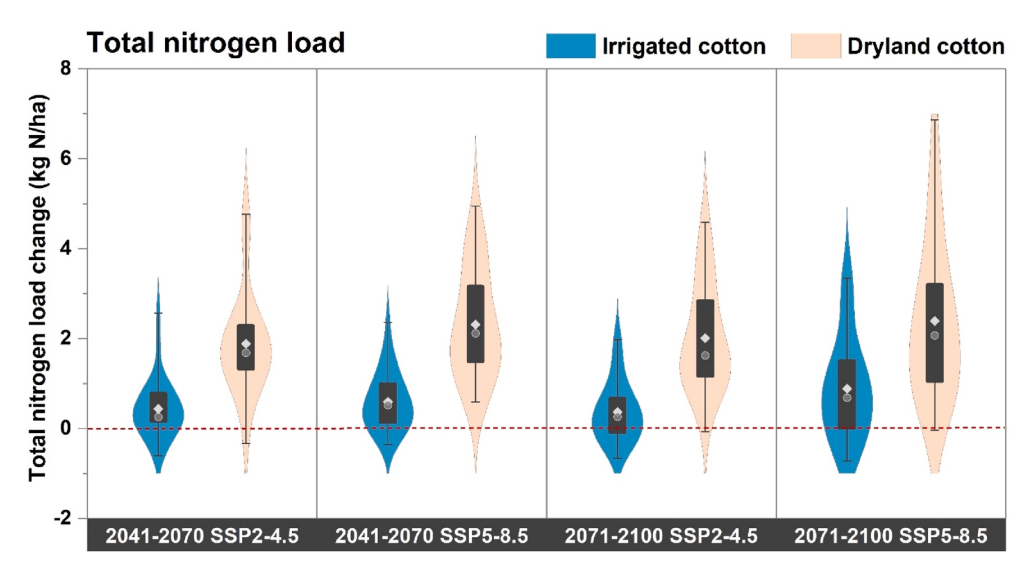


Fig. 4. Changes in total nitrogen load between future and historical periods for 27 GCM models. The blue plots display trends in irrigated cotton and the yellow plots display trends in dryland cotton. Average changes are shown by solid circles, the medians are represented by solid diamonds, whereas minimum, first quartile, third quartile, and maximum are presented as violin plots.

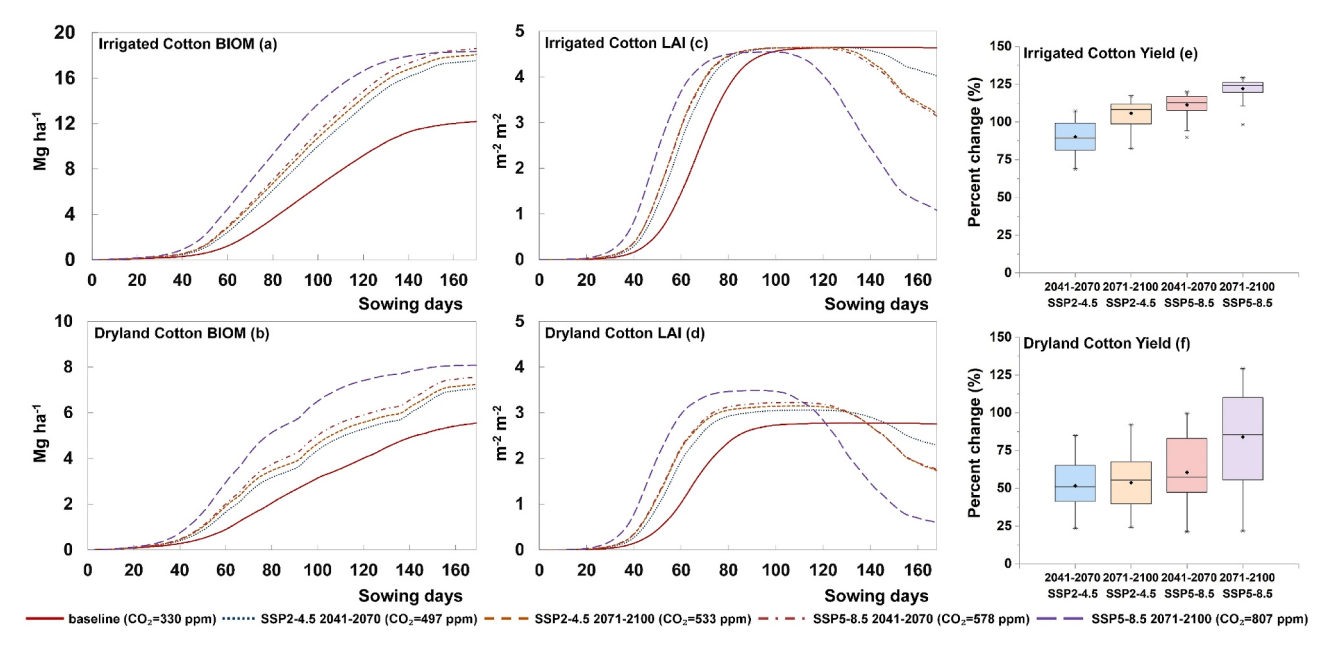


Fig. 5. Changes in irrigated and dryland cotton growth variables of daily biomass (BIOM) values (a and b), daily leaf area index (LAI) values (c and d), and yields (e and f) between future and historical periods for 27 GCM models.

to 5 °C by the mid to late 21st century. Awal et al. (2016) predicted that T_{min} and T_{max} could increase by 2 °C and 3 °C on average in the 2055s and 2090s, respectively, under three greenhouse gas emissions scenarios (A2, A1B, and B1) in the Brazos Headwaters Basin, Texas. Projected climate data used in this study showed that overall future precipitation remained nearly unchanged compared to the baseline. Venkataraman et al. (2016) reported that precipitation could increase in most parts of Texas by the second half of the 21st century under the RCP4.5 scenario, while Herrera-Pantoja and Hiscock (2015) reported a decrease in precipitation in some semi-arid areas. Li et al. (2012) used the data from 36 GCMs and reported the trend of precipitation change for the period 1950-2099 in Houston, Texas; they found that annual average precipitation could decrease apparently under the RCP8.5 scenario but remain relatively constant under the RCP2.6 scenario. In this study, solar radiation was found to increase noticeably by approximately 10%. Other studies also reported similar increasing trends in solar radiation in the future (Rempel et al., 2021; Xiao et al., 2020).

The results from this study showed a decrease (less than 3.5%) in future annual ETa for dryland cotton under the SSP2-4.5 and SSP5-8.5 scenarios. The projected increase in air temperatures did not lead to an increase in ETa, which was consistent with other long-term climate change studies (Dinpashoh et al., 2011; Jhajharia et al., 2015; Venkataraman et al., 2016). Simulated annual ETa for irrigated cotton showed increasing trends under all climate change scenarios, except for the 2071–2100 SSP5-8.5 scenario, which projected a decrease in ET_a by up to 9.3%. The changes in ET_a could be directly or indirectly affected by many factors such as CO₂ concentrations, air temperatures, precipitation, solar radiation, irrigation managment, etc.; therefore, it was difficult to determine which single factor attributed to the changes in ETa. The simulated changes in irrigation water use and ETa by coupling the SWAT-MAD model and GCMs in the study watershed showed similar trends. Moreover, under the 2041-2070 SSP2-4.5, 2071-2100 SSP2-4.5, and 2041-2070 SSP5-8.5 scenarios, the results showed an increase in simulated annual irrigation water use, which was most probably due to the increase in ET_a while holding precipitation relatively constant. However, under the 2071-2100 SSP5-8.5 scenario, the highest CO₂ concentration (807 ppm) was simulated, which led to the partial closure of stomatal apertures and hence inhibited transpiration (Conley et al., 2001; Leuzinger and KÖRner, 2007; Bunce and Nasyrov, 2012). The decrease in ETa in this study would then lead to reductions in the annual

irrigation water use by cotton. The simulated median annual surface runoff for both irrigated and dryland cotton showed evident increases under all four scenarios, with greater increases under dryland conditions. In the irrigated cotton areas, an adequate supply of water and fertilizer would lead to better crop growth and sufficient ground cover. Therefore, under future climate scenarios, precipitation or irrigation water might be trapped by branches and leaves or used mainly for crop transpiration, which would increase the cotton biomass and hence reduce the surface runoff. Accordingly, the changes in TN load were closely correlated to surface runoff, and the increase in surface runoff under future climate scenarios would inevitably increase nitrogen loss from the cotton fields and thus cause surface water pollution (Wei et al., 2021; Hanrahan et al., 2021). Therefore, appropriate mitigation and adaptation strategies need to be implemented to reduce the negative impact of climate change on hydrology and water quality.

The projected climate change caused an increase in simulated cotton lint yield in the DBMF watershed, which was comparable to the results reported in other studies (Adhikari et al., 2016; Kothari et al., 2021), but the magnitude of increase was different. This study showed increases in cotton lint yields in the range of 91.1%-122.1% for irrigated cotton and 47.5%-84.0% for dryland cotton, which were higher than the cotton lint yield change (14%-29% increase) projected in the study of Adhikari et al. (2016) for simulation period of 2041-2070. Other relative parameters such as biomass and LAI were analyzed in this study to investigate possible factors that would influence the cotton lint yield. The simulated maximum biomass yields for both cotton management practices were higher than the biomass yields under the respective baseline scenarios, which supported the findings of increases in cotton lint yields in the future. The changes in simulated LAI under all four climate change scenarios demonstrated that climate change would lead to a shorter growing season in cotton, as higher air temperatures could accelerate maturation and shorten the growth period (Sharma et al., 2021). Cotton plants are heat-tolerant and can grow well within an optimum air temperature range, and low air temperature can adversely affect the cotton lint yield. The accumulated temperature >10 °C might result in a positive effect on the growth and development of cotton and thus influence the final yield (Pettigrew, 2008; Li et al., 2020). Thereby, under the SSP2-4.5 and SSP5-8.5 scenarios, elevated air temperatures promoted increases in cotton lint yield. The natural cotton defoliation during the baseline period was not sufficient to support direct harvesting by machinery. But the early defoliation under the future climate scenarios implied an earlier shedding of cotton leaves, which would potentially reduce the use of defoliants in harvesting and simplify the production processes (Liao et al., 2020).

Due to the complexity of climate change issues and the limitations of human cognition, the projected changes in future climate showed a high variation among different GCMs. There were many causes of uncertainties in climate projections (e.g., downscaling approach, GCM selection, etc.), with the GCM selections being the primary reason for uncertainties in future climate projections (Lee et al., 2021). GCMs have different underlying assumptions, and the more GCMs were selected in a study, the more it could reflect the variety of situations that might occur in the future (Lutz et al., 2016). The newly developed R code can be used to extract and analyze the SWAT outputs more efficiently, and obtain the corresponding changes in hydrology, water quality, and crop growth at yearly, monthly, and daily scales. The R code accurately extracted and organized the data of all 109 scenarios in approximately 24–32 h, which saved a substantial amount of labor and prevented potential errors caused by manual processing. When evaluating the impact of future climate change on regional water resources and crop production, it is important to use more GCMs to capture the uncertainty. With the continuous improvement and increase in the number of GCMs, this R code will become an important post-processing tool for the SWAT users to study climate change impacts on the "Soil-Water-Food" coupling systems.

5. Conclusions

The changes in meteorological variables, water balance components, total nitrogen load, and cotton growth parameters were simulated under changing climate based on 27 CMIP6 GCM projections and a wellcalibrated SWAT-MAD model under four climate change scenarios in the DMFB watershed of the Texas Panhandle. The simulation results demonstrated that air temperatures and solar radiation increased under future climate scenarios, while the precipitation slightly decreased. In future climate scenarios, ETa declined during the dryland cotton growing season. However, in the irrigated cotton growing season, only in the 2071-2100 SSP5-8.5 scenario, the amount of irrigation and ETa showed a downward trend, and the median values of the reductions were 16.3% and 11.2%, respectively. The irrigation amount and ETa in the growing season of irrigated cotton under the other three scenarios showed an upward trend, and the median percentage changes were 3.2%-7.5% and 0.2%-1.9%, respectively. Clearly elevated CO₂ concentration was the major factor for the decrease in ETa and irrigation under the 2071-2100 SSP5-8.5 scenario. In addition, both surface runoff and TN load increased for two cotton management practices under the four climate scenarios, which increased the risk of non-point source pollution in the watershed. Both cotton yields were expected to increase under the four climate change scenarios, and the average annual increase in irrigated cotton yield was nearly double compared to that of dryland cotton yield. Predicting potential ecological and environmental threats in the watershed in the future enable making scientific and reasonable decisions on production and ecological protection for watershed management agencies. The use of the newly developed R code has greatly improved the processing capabilities for long-term, multi-scenario, and multi-variable SWAT-MAD output results, and it can serve as a useful tool and provide technical support for efficiently studying the future climate change impacts.

Software availability

Name of software: SWAT post-processing R tool.

Description: The SWAT post-processing R tool was developed for batch processing of SWAT outputs of the future climate change scenarios, allowing for flexibility to obtain the climate, hydrological, water quality, and crop growth variables of the SWAT model from output.hru

for different time steps (daily, monthly, and yearly).

Developers: Haipeng Liu and Yong Chen.

Year available: 2022.

Availability and Cost: Open source.

Language: R.

Funding

This research was supported by the Chinese Universities Scientific Fund under award numbers 1191–15051002; 1191–15052008; 1191–10092004; and 1191–31051204. The research was also partially supported by the National Institute of Food and Agriculture, U.S. Department of Agriculture under award numbers NIFA-2021-67019-33684 and NIFA-2012-67009-19595.

Declaration of competing interest

The authors declare that they have no known competing financial interests or personal relationships that could have appeared to influence the work reported in this paper.

Acknowledgements

This research was supported in part by the Ogallala Aquifer Program, a consortium between USDA-Agricultural Research Service, Kansas State University, Texas A&M AgriLife Research, Texas A&M AgriLife Extension Service, Texas Tech University, and West Texas A&M University.

Appendix A. Supplementary data

Supplementary data to this article can be found online at https://doi.org/10.1016/j.envsoft.2022.105492.

References

- Abbott, M.B., Refsgaard, J.C., 1996. Distributed Hydrological Modelling. Springer Netherlands. Distributed Hydrological Modelling. SpringerLink.
- Adhikari, P., Ale, S., Bordovsky, J.P., Thorp, K.R., Modala, N.R., Rajan, N., Barnes, E.M., 2016. Simulating future climate change impacts on seed cotton yield in the Texas High Plains using the CSM-CROPGRO-Cotton model. Agric. Water Manag. 164, 317–330, https://doi.org/10.1016/j.agwat.2015.10.011.
- Al-Mukhtar, M., Dunger, V., Merkel, B., 2014. Assessing the impacts of climate change on hydrology of the upper reach of the spree river: Germany. Water Resour. Manag. 28 (10), 2731–2749. https://doi.org/10.1007/s11269-014-0675-2.
- Arnell, N.W., Reynard, N.S., 1996. The effects of climate change due to global warming on river flows in Great Britain. J. Hydrol. 183 (3-4), 397–424. https://doi.org/ 10.1016/0022-1694(95)02950-8.
- Arnold, J.G., Moriasi, D.N., Gassman, P.W., Abbaspour, K.C., White, M.J., Srinivasan, R., Santhi, C., Harmel, R.D., van Griensven, A., Van Liew, M.W., Kannan, N., Jha, M.K., 2012. SWAT: model use, calibration, and validation. Trans. ASABE (Am. Soc. Agric. Biol. Eng.) 55 (4), 1491–1508. https://doi.org/10.13031/2013.42256.
- Arnold, J.G., Srinivasan, R., Muttiah, R.S., Williams, J.R., 1998. Large-area hydrologic modeling and assessment: Part I. Model development. J. Am. Water Resour. Assoc. 34 (1), 73–89. https://doi.org/10.1111/j.1752-1688.1998.tb05961.x.
- Asseng, S., Martre, P., Maiorano, A., et al., 2019. Climate change impact and adaptation for wheat protein. Global Change Biol. 25 (1), 155–173. https://doi.org/10.1111/ gcb.14481.
- Awal, R., Bayabil, H.K., Fares, A., 2016. Analysis of potential future climate and climate extremes in the Brazos Headwaters Basin. Texas. Water 8 (12). https://doi.org/ 10.1016/j.envexpbot.2011.11.015.
- Bunce, J.A., Nasyrov, M., 2012. A new method of applying a controlled soil water stress, and its effect on the growth of cotton and soybean seedlings at ambient and elevated carbon dioxide. Environ. Exp. Bot. 77, 165–169. https://doi.org/10.3390/w8120603.
- Chen, J., Brissette, F.P., Lucas-Picher, P., Caya, D., 2017. Impacts of weighting climate models for hydro-meteorological climate change studies. J. Hydrol. 549, 534–546. https://doi.org/10.1016/j.jhydrol.2017.04.025.
- Chen, Y., Marek, G.W., Marek, T.H., Brauer, D.K., Srinivasan, R., 2018a. Improving SWAT auto-irrigation functions for simulating agricultural irrigation management using long-term lysimeter field data. Environ. Model. Software 99, 25–38. https:// doi.org/10.1016/i.envsoft.2017.09.013.
- Chen, Y., Marek, G.W., Marek, T.H., Moorhead, J.E., Heflin, K.R., Brauer, D.K., Gowda, P. H., 2018b. Assessment of alternative agricultural land use options for extending the

- availability of the Ogallala Aquifer in the Northern High Plains of Texas. Hydrol. 5 (4) https://doi.org/10.3390/hydrology5040053.
- Colaizzi, P.D., Gowda, P.H., Marek, T.H., Porter, D.O., 2009. Irrigation in the Texas High Plains: a brief history and potential reductions in demand. Irrigat. Drain. 58 (3), 257–274. https://doi.org/10.1002/ird.418.
- Conley, M.M., Kimball, B.A., Brooks, T.J., Pinter, P.J., Hunsaker, D.J., Wall, G.W., Adam, N.R., LaMorte, R.L., Matthias, A.D., Thompson, T.L., Leavitt, S.W., Ottman, M.J., Cousins, A.B., Triggs, J.M., 2001. CO₂ enrichment increases water-use efficiency in sorghum. New Phytol. 151 (2), 407–412. https://doi.org/10.1046/ i.1469-8137.2001.00184.x.
- Dinpashoh, Y., Jhajharia, D., Fakheri-Fard, A., Singh, V.P., Kahya, E., 2011. Trends in reference crop evapotranspiration over Iran. J. Hydrol. 399 (3–4), 422–433. https://doi.org/10.1016/j.jhydrol.2011.01.021.
- Faramarzi, M., Abbaspour, K.C., Vaghefi, S.A., Farzaneh, M.R., Zehnder, A.J.B., Srinivasan, R., Yang, H., 2013. Modeling impacts of climate change on freshwater availability in Africa. J. Hydrol. 480, 85–101. https://doi.org/10.1016/j. ihydrol.2012.12.016.
- Gleick, P.H., 1989. Climate change, hydrology, and water resources. Rev. Geophys. 27 (3), 329–344. https://doi.org/10.1029/RG027i003p00329.
- Hanrahan, B.R., King, K.W., Duncan, E.W., Shedekar, V.S., 2021. Cover crops differentially influenced nitrogen and phosphorus loss in tile drainage and surface runoff from agricultural fields in Ohio, USA. J. Environ. Manag. 293, 112910 https://doi.org/10.1016/j.jenvman.2021.112910.
- Herrera-Pantoja, M., Hiscock, K.M., 2015. Projected impacts of climate change on water availability indicators in a semi-arid region of central Mexico. Environ. Sci. Pol. 54, 81–89. https://doi.org/10.1016/j.envsci.2015.06.020.
- Hosseini, P., Bailey, R.T., 2022. Investigating the controlling factors on salinity in soil, groundwater, and river water in a semi-arid agricultural watershed using SWAT-Salt. Sci. Total Environ. 810 https://doi.org/10.1016/j.scitotenv.2021.152293.
- IPCC, 2014. Climate change 2014: Impacts, adaptation, and vulnerability. In: Field, C.B., Barros, V.R., Dokken, D.J., Mach, K.J., Mastrandrea, M.D., Bilir, T.E., White, L.L. (Eds.), Contribution of Working Group II to the Fifth Assessment Report of the Intergovernmental Panel on Climate Change. Cambridge University Press, Cambridge, United Kingdom and New York, NY, USA.
- Jhajharia, D., Kumar, R., Dabral, P.P., Singh, V.P., Choudhary, R.R., Dinpashoh, Y., 2015.
 Reference evapotranspiration under changing climate over the Thar Desert in India.
 Meteorol. Appl. 22 (3), 425–435. https://doi.org/10.1002/met.1471.
- Kothari, K., Ale, S., Bordovsky, J.P., Munster, C.L., Singh, V.P., Nielsen-Gammon, J., Hoogenboom, G., 2021. Potential genotype-based climate change adaptation strategies for sustaining cotton production in the Texas High Plains: a simulation study. Field Crop. Res. 271, 108261 https://doi.org/10.1016/j.fcr.2021.108261.
- Kukal, M.S., Irmak, S., 2018. Climate-driven crop yield and yield variability and climate change impacts on the US Great Plains agricultural production. Sci. Rep. 8, 3450. https://doi.org/10.1038/s41598-018-21848-2.
- Kuti, I.A., Ewemoje, T.A., 2021. Modelling of sediment yield using the soil and water assessment tool (SWAT) model: a case study of the Chanchaga Watersheds, Nigeria. Sci. Afr. 13, e00936 https://doi.org/10.1016/j.sciaf.2021.e00936.
- Lee, S., Qi, J., McCarty, G.W., Yeo, I.Y., Zhang, X., Moglen, G.E., Du, L., 2021. Uncertainty assessment of multi-parameter, multi-GCM, and multi-RCP simulations for streamflow and non-floodplain wetland (NFW) water storage. J. Hydrol. 600, 126564 https://doi.org/10.1016/j.jhydrol.2021.126564.
- Leuzinger, S., KÖRner, C., 2007. Water savings in mature deciduous forest trees under elevated CO₂. Global Change Biol. 13 (12), 2498–2508. https://doi.org/10.1111/i.1365-2486.2007.01467.x
- Li, X., Shi, W., Broughton, K., Smith, R., Sharwood, R., Payton, P., Bange, M., Tissue, D. T., 2020. Impacts of growth temperature, water deficit and heatwaves on carbon assimilation and growth of cotton plants (Gossypium hirsutum L.). Environ. Exp. Bot. 179, 104204 https://doi.org/10.1016/j.envexpbot.2020.104204.
- Li, Z., Zheng, F.L., Liu, W.Z., 2012. Spatiotemporal characteristics of reference evapotranspiration during 1961-2009 and its projected changes during 2011-2099 on the Loess Plateau of China. Agric. For. Meteorol. 154-155, 147–155. https://doi. org/10.1016/j.agrformet.2011.10.019.
- Liao, J., Zang, Y., Luo, X., Zhou, Z., Zang, Y., Wang, P., Hewitt, A.J., 2020. The relations of leaf area index with the spray quality and efficacy of cotton defoliant spraying using unmanned aerial systems (UASs). Comput. Electron. Agric. 169, 105228 https://doi.org/10.1016/j.compag.2020.105228.
- Liu, D., Zuo, H., 2012. Statistical downscaling of daily climate variables for climate change impact assessment over New South Wales, Australia. Clim. Change 115 (3–4), 629–666. https://doi.org/10.1007/s10584-012-0464-y.
- Lutz, A.F., ter Maat, H.W., Biemans, H., Shrestha, A.B., Wester, P., Immerzeel, W.W., 2016. Selecting representative climate models for climate change impact studies: an advanced envelope-based selection approach. Int. J. Climatol. 36 (12), 3988–4005. https://doi.org/10.1002/joc.4608.
- Marras, P.A., Lima, D.C.A., Soares, P.M.M., Cardoso, R.M., Medas, D., Dore, E., De Giudici, G., 2021. Future precipitation in a Mediterranean island and streamflow changes for a small basin using EURO-CORDEX regional climate simulations and the SWAT model. J. Hydrol. 603, 127025 https://doi.org/10.1016/j.ibudrol.2021.127025
- Mehr, A.D., Sorman, A.U., Kahya, E., Afshar, M.H., 2020. Climate change impacts on meteorological drought using SPI and SPEI: case study of Ankara, Turkey. Hydrol. Sci. J. 65 (2), 254–268. https://doi.org/10.1080/02626667.2019.1691218.
- Meinshausen, M., Smith, S.J., Calvin, K., Daniel, J.S., Kainuma, M.L.T., Lamarque, J.F., Matsumoto, K., Montzka, S.A., Raper, S.C.B., Riahi, K., Thomson, A., Velders, G.J.M., van Vuuren, D.P.P., 2011. The RCP greenhouse gas concentrations and their extensions from 1765 to 2300. Clim. Change 109 (1–2), 213–241. https://doi.org/ 10.1007/s10584-011-0156-z.

- Moriasi, D.N., Arnold, J.G., Van Liew, M.W., Bingner, R.L., Harmel, R.D., Veith, T.L., 2007. Model evaluation guidelines for systematic quantification of accuracy in watershed simulations. Trans. ASABE (Am. Soc. Agric. Biol. Eng.) 50 (3), 885–900. https://doi.org/10.13031/2013.23153.
- Nakićenović, N., 1996. Freeing energy from carbon. Daedalus 125 (3), 95-112.
- National Agricultural Statistics Service (NASS), 2020. Irrigation and water management survey. Available online: https://www.nass.usda.gov/Surveys/Guide_to_NASS_Surveys/Farm_and_Ranch_Irrigation/. (Accessed 10 October 2020). accessed on.
- National Agricultural Statistics Service (NASS), 2021. Available online: https://www.nass.usda.gov/. (Accessed 29 July 2021). accessed on.
- Neitsch, S.L., Arnold, J.G., Kiniry, J.R., Williams, J.R., 2011. Soil and Water Assessment Tool Theoretical Documentation Version 2009. Texas Water Resources Institute, Texas. http://swat.tamu.edu/media/99192/swat2009-theory.pdf.
- O'Neill, B.C., Tebaldi, C., van Vuuren, D.P., Eyring, V., Friedlingstein, P., Hurtt, G., Knutti, R., Kriegler, E., Lamarque, J.F., Lowe, J., Meehl, G.A., Moss, R., Riahi, K., Sanderson, B.M., 2016. The scenario model Intercomparison project (ScenarioMIP) for CMIP6. Geosci. Model Dev. (GMD) 9 (9), 3461–3482. https://doi.org/10.5194/gmd-9-3461-2016.
- Papadopoulos, T., Balta, M.E., 2022. Climate Change and big data analytics: challenges and opportunities. Int. J. Inf. Manag. 63, 102448 https://doi.org/10.1016/j. ijinfomgt.2021.102448.
- Pettigrew, W.T., 2008. The effect of higher temperatures on cotton lint yield production and fiber quality. Crop Sci. 48 (1), 278–285. https://doi.org/10.2135/ cropsci2007.05.0261.
- Rempel, A.R., Rempel, A.W., McComas, S.M., Duffey, S., Enright, C., Mishra, S., 2021. Magnitude and distribution of the untapped solar space-heating resource in U.S. climates. Renew. Sustain. Energy Rev. 151, 111599 https://doi.org/10.1016/j.rser.2021.111599.
- Samimi, M., Mirchi, A., Moriasi, D., Ahn, S., Alian, S., Taghvaeian, S., Sheng, Z., 2020. Modeling arid/semi-arid irrigated agricultural watersheds with SWAT: applications, challenges, and solution strategies. J. Hydrol. 590, 125418 https://doi.org/10.1016/j.jhydrol.2020.125418.
- Schlund, M., Lauer, A., Gentine, P., Sherwood, S.C., Eyring, V., 2020. Emergent constraints on equilibrium climate sensitivity in CMIP5: do they mid for CMIP6? Earth Syst. Dyn. 11 (4), 1233–1258. https://doi.org/10.5194/esd-11-1233-2020.
- Sharma, A., Deepa, R., Sankar, S., Pryor, M., Stewart, B., Johnson, E., Anandhi, A., 2021. Use of growing degree indicator for developing adaptive responses: a case study of cotton in Florida. Ecol. Indicat. 124, 107383 https://doi.org/10.1016/j.ecolind.2021.107383
- Shen, M., Chen, J., Zhuan, M., Chen, H., Xu, C.Y., Xiong, L., 2018. Estimating uncertainty and its temporal variation related to global climate models in quantifying climate change impacts on hydrology. J. Hydrol. 556, 10–24. https://doi.org/10.1016/j. ihydrol.2017.11.004.
- Son, N.T., Le Huong, H., Loc, N.D., Phuong, T.T., 2022. Application of SWAT model to assess land use change and climate variability impacts on hydrology of Nam Rom Catchment in Northwestern Vietnam. Environment. Environ. Dev. Sustain. 24, 3091–3109. https://doi.org/10.1007/s10668-021-01295-2.
- Tan, L., Feng, P., Li, B., Huang, F., Liu, D.L., Ren, P., Liu, H., Srinivasan, R., Chen, Y., 2022. Climate change impacts on crop water productivity and net groundwater use under a double-cropping system with intensive irrigation in the Haihe River Basin, China. Agric. Water Manag. 266, 107560 https://doi.org/10.1016/j.agwat.2022.107560.
- van Vuuren, D.P., Den Elzen, M.G.J., Lucas, P.L., Eickhout, B., Strengers, B.J., van Ruijven, B., Wonink, S., van Houdt, R., 2007. Stabilizing greenhouse gas concentrations at low levels: an assessment of reduction strategies and costs. Clim. Change 81 (2), 119–159. https://doi.org/10.1007/s10584-006-9172-9.
- Venkataraman, K., Tummuri, S., Medina, A., Perry, J., 2016. 21st century drought outlook for major climate divisions of Texas based on CMIP5 multimodel ensemble: implications for water resource management. J. Hydrol. 534, 300–316. https://doi. org/10.1016/j.jhydrol.2016.01.001.
- Vesco, P., Kovacic, M., Mistry, M., Croicu, M., 2021. Climate variability, crop and conflict: exploring the impacts of spatial concentration in agricultural production. J. Peace Res. 58 (1), 98–113. https://doi.org/10.1177/0022343320971020.
- Wagner-Riddle, C., Congreves, K.A., Abalos, D., Berg, A.A., Brown, S.E., Ambadan, J.T., Gao, X., Tenuta, M., 2017. Globally important nitrous oxide emissions from croplands induced by freeze-thaw cycles. Nat. Geosci. 10 (4), 279–283. https://doi. org/10.1038/NGE02907.
- Wang, Q., Qi, J., Li, J., Cole, J., Waldhoff, S.T., Zhang, X., 2020. Nitrate loading projection is sensitive to freeze-thaw cycle representation. Water Res. 186, 116355 https://doi.org/10.1016/j.watres.2020.116355.
- Wei, Z., Hoffland, E., Zhuang, M., Hellegers, P., Cui, Z., 2021. Organic inputs to reduce nitrogen export via leaching and runoff: a global meta-analysis. Environ. Pollut. 291, 118176 https://doi.org/10.1016/j.envpol.2021.118176.
- Wilby, R.L., Harris, I., 2006. A framework for assessing uncertainties in climate change impacts: low-flow scenarios for the River Thames, UK. Water Resour. 42 (2), W02419 https://doi.org/10.1029/2005WR004065.
- Wing, I.S., Cian, E.D., Mistry, M.N., 2021. Global vulnerability of crop yields to climate change. J. Environ. Econ. Manag. 109, 102462 https://doi.org/10.1016/j. jeem.2021.102462.
- Xiao, D., Liu, D.L., Wang, B., Feng, P., Bai, H., Tang, J., 2020. Climate change impact on yields and water use of wheat and maize in the North China Plain under future climate change scenarios. Agric. Water Manag. 238, 106238 https://doi.org/ 10.1016/j.agwat.2020.106238.
- Yun, X., Tang, Q., Li, J., Lu, H., Zhang, L., Chen, D., 2021. Can reservoir regulation mitigate future climate change induced hydrological extremes in the Lancang-

Mekong River Basin? Sci. Total Environ. 785, 147322 https://doi.org/10.1016/j.scitatenv.2021.147322

Zhang, J., Lu, C., Feng, H., Hennessy, D., Guan, Y., Wright, M.M., 2021. Extreme climate increased crop nitrogen surplus in the United States. Agric. For. Meteorol. 310, 108632 https://doi.org/10.1016/j.agrformet.2021.108632.

Zhang, R., Cheng, L., Liu, P., Huang, K., Gong, Y., Qin, S., Liu, D., 2021. Effect of GCM credibility on water resource system robustness under climate change based on decision scaling. Adv. Water Resour. 158, 104063 https://doi.org/10.1016/j.advwatres.2021.104063.